Subregional slicing method to increase three-dimensional nanofabrication efficiency in two-photon polymerization

Sang Hu Park, Sang Ho Lee,[a] and Dong-Yol Yang[b]
Department of Mechanical Engineering, Korea Advanced Institute of Science and Technology, Daejeon 305-701, Korea

Hong Jin Kong
Department of Physics, Korea Advanced Institute of Science and Technology, Daejeon 305-701, Korea

Kwang-Sup Lee
Department of Polymer Science and Engineering, Hannam University, Daejeon 306-791, Korea

(Received 1 June 2005; accepted 23 August 2005; published online 7 October 2005)

A subregional slicing method (SSM) is proposed to increase the nanofabrication efficiency of a nanostereolithography (NSL) process based on two-photon polymerization (TPP). The NSL process can be used to fabricate three-dimensional (3D) microstructures via the accumulation of layers of uniform thickness; hence, the precision of the final 3D microstructure depends on the layer thickness. The use of a uniform layer thickness means that, to fabricate a precise microstructure, a large number of thin slices is inevitably required, leading to long processing times. In the SSM proposed here, however, the 3D microstructure is divided into several subregions on the basis of the geometric slope, and then each of these subregions is uniformly sliced with a layer thickness determined by the geometric slope characteristics of each subregion. Subregions with gentle slopes are sliced with thin layer thicknesses, whereas subregions with steep slopes are sliced with thick layer thicknesses. Here, we describe the procedure of the SSM based on TPP, and discuss the fabrication efficiency of the method through the fabrication of a 3D microstructure. © *2005 American Institute of Physics*. [DOI: 10.1063/1.2103393]

Numerous nanofabrication processes have been investigated,[1–5] most of which are capable of fabricating two-dimensional (2D) nanopatterns and simple three-dimensional (3D) microstructures; however, the resolution of features fabricated using photolithographic methods is limited by optical diffraction. Additionally, most of the processes developed to date do not allow the fabrication of arbitrary 3D microstructures. Currently, the only nanofabrication process capable of 3D microfabrication is two-photon polymerization (TPP), which has been successfully used to produce 3D structures in diverse applications such as photonic crystals,[6] optical memories,[7] and micromechanical devices.[8] Two-photon absorption (TPA) itself has been also of considerable interest in the study of novel nonlinear-optical phenomena for a long time.[9]

The basis of TPP is the conversion of a liquid-state resin to a solid phase by photopolymerization, where the polymerization is initiated by exposure of focused high-intensity light into the volume of resins. The quadratic dependence of polymerization rate on light intensity enables control of polymerization with 3D spatial resolution at a resolution better than the diffraction limit of the beam, which may be difficult to attain using conventional single photon lithography processes. In fact, a lateral spatial resolution of close to 100 nm has been reported.[10] Recent work in this area has explored the use of TPP to fabricate 3D microstructures utilizing various materials with properties tailored to specific applications, such as biocompatible materials,[11] polymers doped with nanoparticles for increasing the index of refraction in photonic crystals,[12] and a poly-dimethylsiloxane-based resin for the fabrication of microfluidic devices.[13]

In our work, a titanium sapphire laser operated in mode-locked at 80 MHz and 780 nm wavelength with pulses of duration less than 100 fs was utilized as the light source. A set of two-galvano mirror was used to move the focused laser beam delicately in the horizontal plane, and a piezoelectric stage was used for the vertical alignment of the beam. The laser was closely focused into the volume of the resin which is dropped on a thin glass plate using a high numerical aperture (1.4, immersion oil used) objective lens. A high-magnification charge-coupled-device camera was used for the optical adjustment of the focused beam and monitoring the fabrication process.

The TPA resin used in this work was a mixture of a commercial urethane acrylate resin (SCR500, JSR) and an additional photosensitizer (TP-Flu-TP2, 0.1 wt %) that was synthesized from 2,7-dibromo-9,9-diethylhexyl-9H-fluorene and diphenyl(4-vinylphenyl) amine.[14] It has a large light absorbance and transfers the excited fluorescent light to the initiator for polymerization. Its TPA cross section was found to be 954 GM ($1\ \mathrm{GM}=1\times10^{-50}\ \mathrm{cm}^4\ \mathrm{s/photon}$) at a wavelength of 940 nm. The absorption and fluorescence wavelengths of the photosensitizer were 411 and 472 nm, respectively.[15–17]

In many previous works, complex 3D microstructures have been fabricated by the sequential accumulation of polymerized 2D layers of the same thickness.[8,10,11,17] Therefore, the precision of the resulting 3D microstructures depends on the layer thickness. For precise 3D microfabrication, a small layer thickness is essential, but necessitates large quantities of data and very long processing times. In the uniform slicing method (USM), the appropriate slicing thickness is de-

[a]Present address: LG-PRC, LG Electronics, Jinwi-myeon, Pyeongtaek-si, Gyeonggi-do 451-713, Korea.
[b]Author to whom correspondence should be addressed; electronic mail: dyyang@kaist.ac.kr

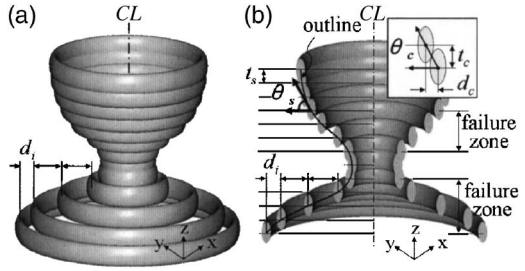

FIG. 1. (a) Schematic diagram of an axisymmetric structure fabricated by layer-by-layer accumulation of multiple layers of the same thickness; d_i represents a horizontal distance between the upper and lower contours, and CL is the center-line of the structure. (b) A sectional diagram of the structure, clearly showing the failure in the accumulation of layers in the gentle slope region due to use of too large a slicing thickness; t_s represents the slicing layer thickness; and θ_c, t_c, and d_c are the critical slope, the critical slicing thickness, and the critical horizontal distance, respectively.

termined by considering the minimum geometric slope and the complexity of the 3D microstructure. If the 3D microstructure has gentle local slopes, the slicing thickness, determined by the minimum local slope, will be very thin. Moreover, a 3D microstructure in which regions with steep slopes predominate, but which contains some regions with gentle local slopes, will have to be sliced throughout with thin slices suitable for the gentle slope region; therefore, the USM is not an effective method for fabricating 3D microstructures.

If a microstructure with gentle slopes is sliced using thick uniform layers to reduce the total number of layers, the surface in the gentle slope regions may be scabrous; moreover, in some cases this approach will lead to failure of the fabrication of the microstructure due to the separation of layers in the gentle slope regions. The schematic diagrams in Figs. 1(a) and 1(b) outline the criterion for failure due to the separation of layers that occurs when the slicing thickness (t_s) exceeds a certain critical value (t_c); in this case, a horizontal distance between the upper and lower contours (d_i) is larger than a critical horizontal distance (d_c). The critical thickness t_c is a function of the slope of the outline (θ_s) and the geometric section of the contour layers, which is determined by the fabrication conditions, such as the laser power and exposure time;[10,11,17] t_c is achieved using the critical slope (θ_c) that is determined by the d_c, as illustrated in the inset of Fig. 1(b). Also, for a given slicing thickness in the USM, the critical slope, θ_c, in the designed microstructure can also be obtained using the same way.

Here, we describe our results on increasing the fabrication efficiency by using a subregional slicing method (SSM) in the TPP process. In the SSM procedure, the computer aided device (CAD) program Nano-Slicer[17] is used to divide a 3D microstructure into several subregions on the basis of its geometric shape or critical slopes, and then a suitable slicing thickness is applied to each subregion of the microstructure. Compared with the USM method, the SSM approach enables the fabrication of microstructures using fewer layers but with greater precision.

To obtain critical slopes according to several layer thicknesses, we attempted to fabricate hemispheres of diameter 15 μm using a slicing thickness of 30, 50, 100, 150, or 200 nm. The slope of the outline of the hemisphere ranges from 0 to 90 deg. The procedure for generating the data for each hemisphere was as follows: (1) the designed hemisphere was transformed to the stereolithography (STL) format,[18] which has been utilized widely in the rapid prototyping process; (2) the hemisphere was sliced utilizing the intersection points between slicing planes and triangular patches of the STL format, as shown in Fig. 2(a); and (3) the data for the 2D scanning paths of the laser beam were constructed using the sliced contour data. Figures 2(c) and 2(d) show scanning electron microscopy (SEM) images of hemispheres fabricated under conditions of laser power, 60 mW and exposure time, 1 ms. The contour linewidth and height generated under these experimental conditions are known to be approximately 180 and 580 nm, respectively, from preliminary tests.[17] A critical length (L_c) was measured using the top-view SEM images [Fig. 2(c)] to geometrically calculate the critical slopes for each slicing thickness. We included a failure zone and a scabrous surface into the calculation of the critical length, L_c, as defined in Figs. 2(b) and 2(c). The experiments showed that a near-perfect hemisphere was fabricated using a slicing thickness of 30 nm, and the critical slopes obtained for the various slicing thicknesses were 9.75° at 30 nm, 20.52° at 50 nm, 27.18° at 100 nm, 34.67° at 150 nm, and 49.20° at 200 nm. In this work, the failure-proof range of slopes (for laser power 60 mW and exposure time 1 ms) was divided into six regions within an acute angle using the critical slopes as follows: region 1 (0°–9.75°), region 2 (9.76°–20.52°), region 3 (20.53°–27.18°), region 4 (27.19°–34.67°), region 5 (34.68°–49.20°), and region 6 (49.21°–90°), and their corresponding slicing thicknesses were less than 30, 30, 50, 100, 150, and 200 nm, respectively.

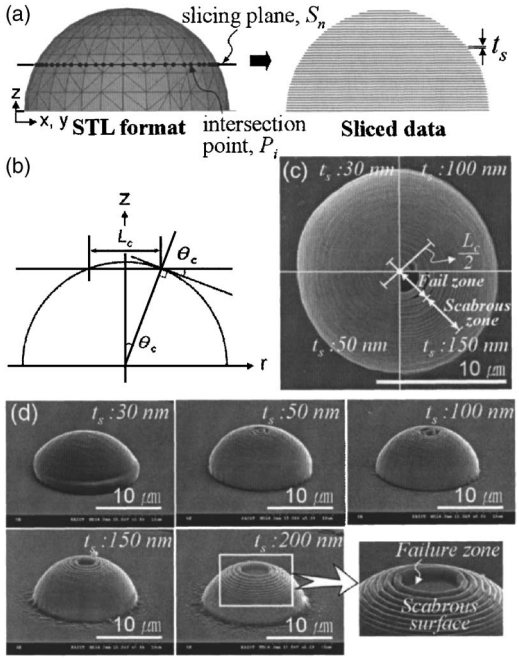

FIG. 2. (a) STL format of a hemisphere and intersection point, P_i, with slicing plane, S_n, and its slicing data for uniform slicing into layers of thickness, t_s. (b) Schematic diagram for the calculation of slopes, θ_s, by an analytical method; L_c represents the critical length, which is measured from the top view of SEM images of the hemispheres. (c) Combined SEM image showing quarter parts of the hemispheres fabricated using four slicing thicknesses, respectively, under fabrication conditions of laser power 60 mW and exposure time 1 ms. Each line on the SEM image represents the half of critical length, $L_c/2$, including the length of failure zone and scabrous zone. (d) SEM images of the fabricated hemispheres with various slicing thicknesses from 30 to 200 nm (inclined view).

The fabrication efficiency of the proposed SSM was experimentally examined by means of the fabrication of a mi-

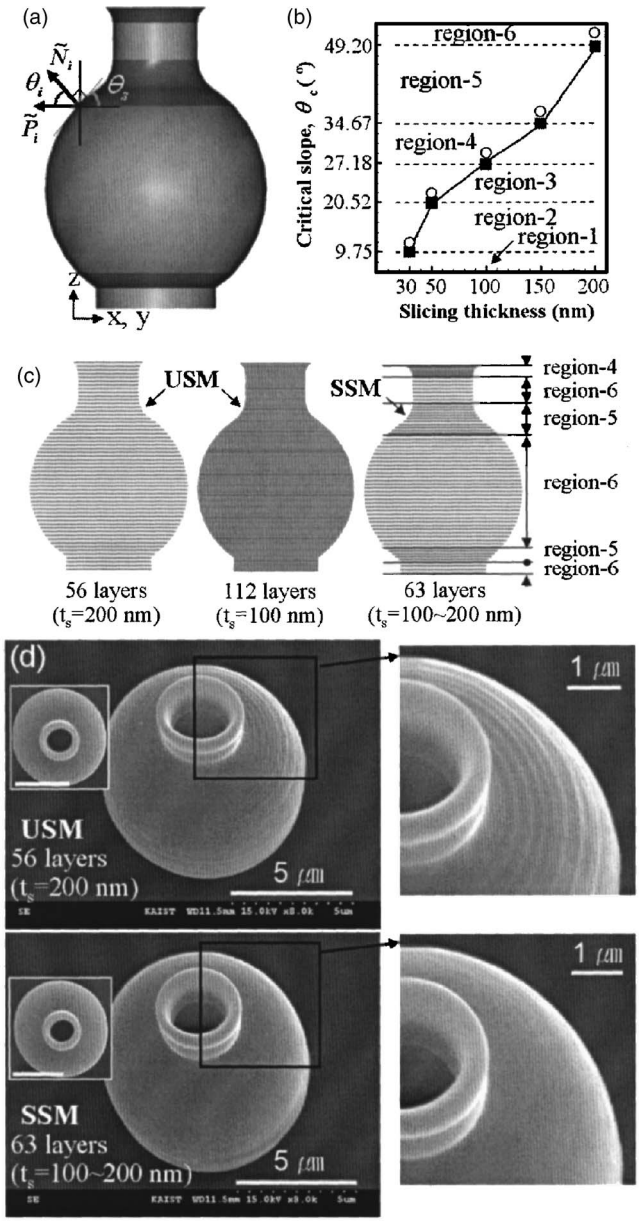

FIG. 3. (a) Designed CAD data and definitions of the normal vector ($\tilde{N}_i$), plane component of the normal vector ($\tilde{P}_i$), and the angle of the slope (θ_s). (b) Variation of the critical slope (θ_c) obtained under the laser power of 60 mW and exposure time of 1 ms (■), and under the laser power of 40 mW and exposure time of 1 ms (○) according to the slicing thickness. (c) Three types of sliced data: 56 layers of uniform thickness 200 nm sliced using the uniform slicing method (USM), 112 layers of uniform thickness 100 nm sliced using the USM; and 63 layers sliced using the SSM. (d) SEM images of microjars fabricated using the USM with 56 layers, and the SSM with 63 layers (inset images: top view of each microjar, scale bar is 5 μm).

crojar. Figure 3(a) shows the microjar, which was designed using a CAD tool. The slope of a 3D microstructure along the outline, θ_s, can be obtained using the following simple vector equation:

$$\theta_s = \frac{\pi}{2} - \theta_i = \frac{\pi}{2} - \cos^{-1}\frac{\tilde{N}_i \cdot \tilde{P}_i}{|\tilde{N}_i||\tilde{P}_i|}, \tag{1}$$

where θ_i are the angles between the normal vectors of the outlines, $\tilde{N}_i(\tilde{n}_x\ \tilde{n}_y\ \tilde{n}_z)$, and the projected vectors of normal vectors onto the slicing planes, $\tilde{P}_i$, as depicted in Fig. 3(a).

The slopes of the microjar outline ranged from 29.5° to 90°; therefore, from the results of the preliminary tests shown in Fig. 3(b), the microjar could be fabricated without any defects using a slicing thickness of 100 nm under a laser power of 60 mW and exposure time of 1 ms. Figure 3(c) shows the slice configurations of the microjar for the USM and SSM. For the USM, there were 112 layers of thickness 100 nm for the perfect fabrication or 56 layers of thickness 200 nm for the fabrication without failure zone, respectively. For the SSM, by contrast, there were 63 layers divided into six subregions with slicing thicknesses of 100, 150, and 200 nm respectively. Figure 3(d) shows SEM images of the microjar fabricated by the USM with 56 layers of thickness 100 nm (upper images) and the microjar fabricated using SSM (lower images). The microjar fabricated using the USM has a rough surface in the gentle ascent region, whereas the microjar fabricated using the SSM has a smoother surface even though it was fabricated in a similar time. The microjar fabricated using the USM with 112 layers of uniform slicing thickness 100 nm had a similar precision to that of the microjar fabricated using the SSM; however, the fabrication time was taken about twice that required using the SSM due to the large slice data.

In conclusion, we have shown that the precision of 3D microstructures fabricated using the TPP process, as well as the fabrication efficiency, are very sensitive to the slicing thickness. To fabricate a precise microstructure, the uniform slicing layer thickness must be determined on the basis of the gentlest local slope of the microstructure. This requirement means that many slices are required in the USM. If, however, different slicing thicknesses are applied in different subregions of the microstructure by utilizing the SSM, the fabrication efficiency is improved and the processing time is substantially reduced. The present findings underline the benefits of using the SSM in the fabrication of complex 3D microstructures using the TPP.

[1] S. Y. Chou, P. R. Krauss, and P. J. Renstrom, Science **272**, 85 (1996).
[2] Y. Xia, J. Tien, D. Qin, and G. M. Whitesides, Langmuir **12**, 4033 (1996).
[3] M. D. Austin, H. Ge, W. Wu, M. Li, Z. Yu, D. Wasserman, S. A. Lyon, and S. Y. Chou, Appl. Phys. Lett. **84**, 5299 (2004).
[4] R. D. Piner, J. Zhu, F. Xu, S. Hong, and C. A. Mirkin, Science **283**, 661 (1999).
[5] C. M. Bruinink, M. Peter, M. Boer, L. Kuipers, J. Huskens, and D. N. Reinhoudt, Adv. Mater. (Weinheim, Ger.) **16**, 1086 (2004).
[6] H.-B. Sun, V. Mizeikis, Y. Xu, S. Juodkazis, J.-Y. Ye, S. Matsuo, and H. Misawa, Appl. Phys. Lett. **79**, 3173 (2001).
[7] A. S. Dvornikov and P. M. Rentzepis, Opt. Commun. **119**, 341 (1995).
[8] H.-B. Sun, K. Takada, and S. Kawata, Appl. Phys. Lett. **79**, 3173 (2001).
[9] W. L. Peticolas, J. P. Goldsborough, and K. E. Rieckhoff, Phys. Rev. Lett. **10**, 43 (1963).
[10] H.-B. Sun, K. Tanaka, M.-S. Kim, K.-S. Lee, and S. Kawata, Appl. Phys. Lett. **83**, 1104 (2003).
[11] J. Serbin, A. Egbert, A. Ostendorf, B. N. Chichkov, R. Houbertz, G. Domann, J. Schulz, C. Cronauer, L. Frohlich, and M. Popall, Opt. Lett. **28**, 301 (2003).
[12] X. M. Duan, H. B. Sun, K. Kaneko, and S. Kawata, Thin Solid Films **453**, 518 (2004).
[13] C. A. Coenjarts and C. K. Ober, Chem. Mater. **16**, 5556 (2004).
[14] H. K. Yang, Master thesis, Hannam University, Korea, 2003.
[15] T. W. Lim, S. H. Park, and D. Y. Yang, Microelectron. Eng. **77**, 382 (2005).
[16] S. H. Park, T. W. Lim, D. Y. Yang, H. J. Kong, K. S. Kim, and K.-S. Lee, Bull. Korean Chem. Soc. **25**, 1119 (2004).
[17] S. H. Park, T. W. Lim, S. H. Lee, D. Y. Yang, H. J. Kong, and K.-S. Lee, Polymer (Korea) **29**, 146 (2005).
[18] P. F. Jacobs, *Stereolithography and Other RP&M Technologies* (ASME, New York, 1996), p. 123.